technical memorandum

Daresbury Laboratory

DL/SCI/TM89E

RAYTRACING RESULTS FOR BEAMLINE 6.1

by

F.M. QUINN and P. BAILEY, SERC Daresbury Laboratory.

DECEMBER, 1992

G92/247

Science and Engineering Research Council
DARESBURY LABORATORY
Daresbury, Warrington WA4 4AD

ISSN 0144-5677

Raytracing Results for Beamline 6.1

F.M. Quinn, P. Bailey

Daresbury Laboratory

Abstract

The optical system of the plane grating monochromator on beamline 6.1 was studied using a raytracing program called SHADOW. The results are presented here in some detail as an example of some of the capabilities of the program. The predictions for the resolution are also compared to data taking during a period of commissioning. These are in reasonable agreement, indicating that the monochromator is now correctly configured to produce the best focus possible over the most frequently used photon energy range.

Contents

1. Introduction

Although the plane grating monochromator on VUV6.1 is the oldest on site, it still presents an interesting example for optimising optical systems. The designs of several recent monochromators are based on the use of plane gratings and spherical focussing optics but differ in the prefocussing mirrors[1]. This document outlines the results of raytracing the optical system using SHADOW[2] and compares these with the most recent benchmarking data obtained during commissioning.

1.1. System description

Briefly, the beamline accepts 8mrads horizontally from the shield wall side of the fan of light from magnet 6. This is collected and horizontally focused by a cylindrical, horizontally deflecting SiC mirror. The plane grating monochromator is self-contained in a single vessel and consists of a variable entrance aperture, a plane grating, and a spherical mirror which produces a vertical and horizontal focus at the exit slits. There are two spherical mirrors of radii 4206 and 3250mm in the monochromator vessel and selection is made by varying the mirror carriage position. The light is then horizontally and vertically focused to a small spot in the experimental chamber by a horizontally deflecting ellipsoidal mirror. The system is shown in figure 1 and further details tabulated in appendix 1.

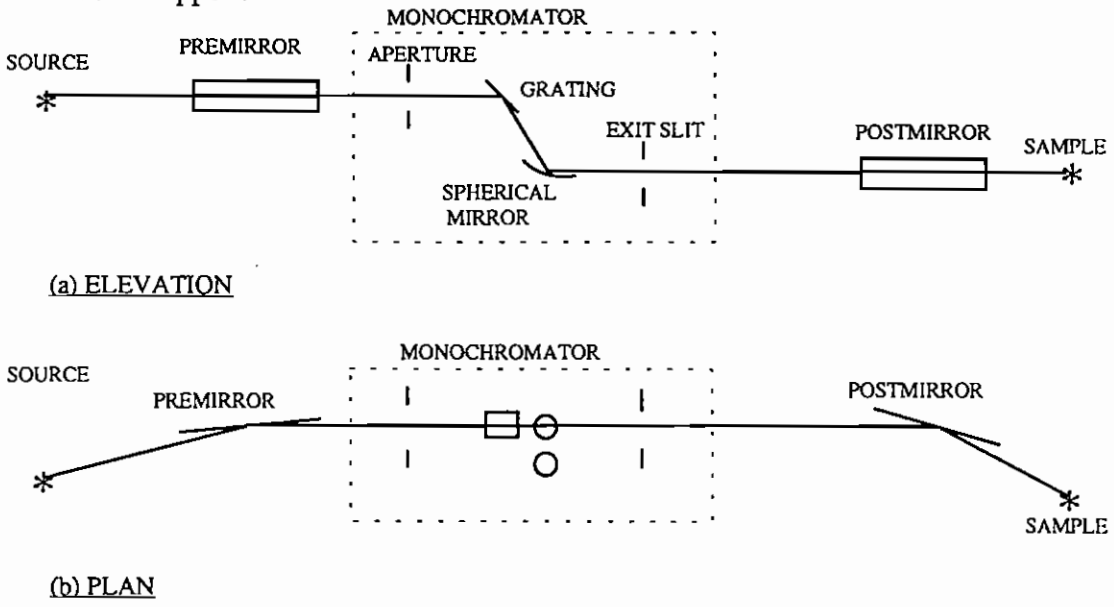

Figure 1. Arrangement of optical elements in VUV6.1

2. SHADOW

SHADOW is a ray tracing programme which can generate a synchrotron radiation source in the form of a ray file where each ray has a defined energy, phase/direction, position and intensity. This source can be random in real and momentum space or in the form of a grid. The energy distribution in a source file can be continuous over a specified range, contain several discrete values or a single energy value. The source used for the following calculations was random and with the appropriate energy distribution for the calculation in hand.

The programme is capable of dealing with most mirror shapes such as plane, cylindrical, spherical, elliptical or toroidal and each ray's position as it intercepts either a mirror surface or a specified image plane can be plotted.

The version used to obtain the results here is version 89.3 and runs on VAX A. The ease of use of this version is limited by the graphics package used (TOPDRAWER).

2.1. SHADOW images

The raytracing programme produces several different image files. The routine SYSPLOT can give 3D and 2D traces of the system. These plots are shown in figure 2(a) to (c). In this study, their main use has been to show that the optical description used is correct. It is easy to get mirror orientations wrong. The quality of the image is limited by using a screen dump process to save the image. However, this is not critical as their use is debatable.

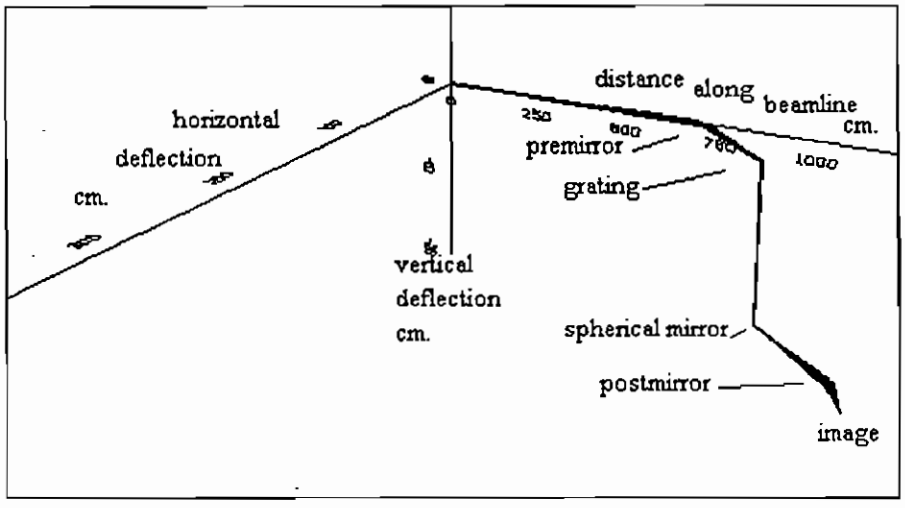

Figure 2(a) Three dimensional system plot using 200 rays

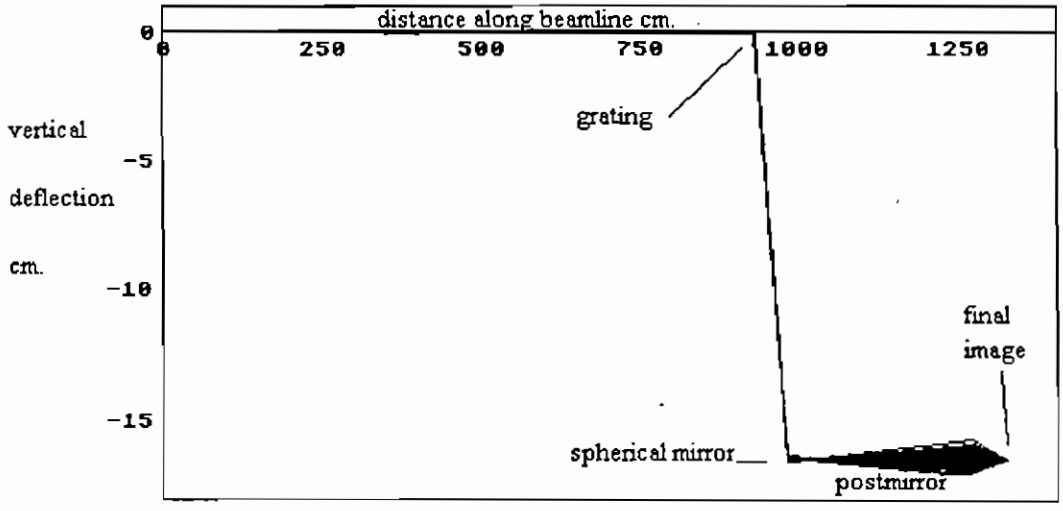

Figure 2(b) Two dimensional system plot showing vertical deflection

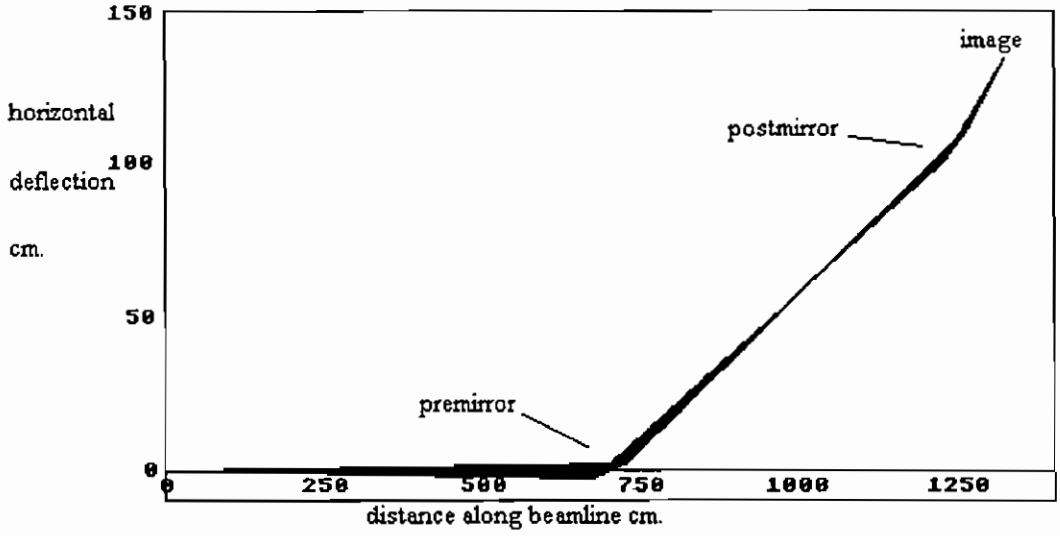

Figure 2(c) Two dimensional system plot showing horizontal deflection

Once the optical system has been specified correctly, the images produced at key points along the optical path can be displayed using PLOTXY to look at the image files (STAR.NN) and to look at the footprints on the optical elements (MIRR.NN). These show the position of each ray as it intercepts the specified image plane or the mirror surface. Also shown in the output from PLOTXY are the vertical and horizontal ray distributions in the form of histograms on the relevant axes. The scale is defined in an information box on the right of the plot. The units used throughout this study are centimetres. The plots for VUV6.1 are shown in figures 3 (a) to (g) for 140eV photons. The zero order angle was 81.488^{o} (see section 3). These are similar to the visible footprints.

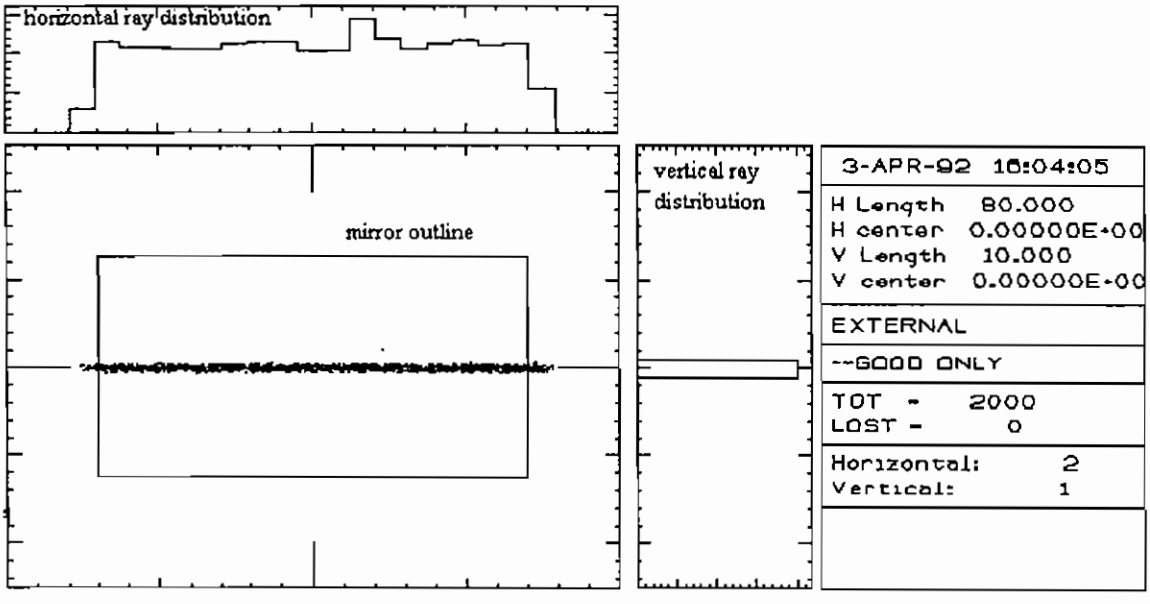

Figure 3(a) Footprint on premirror

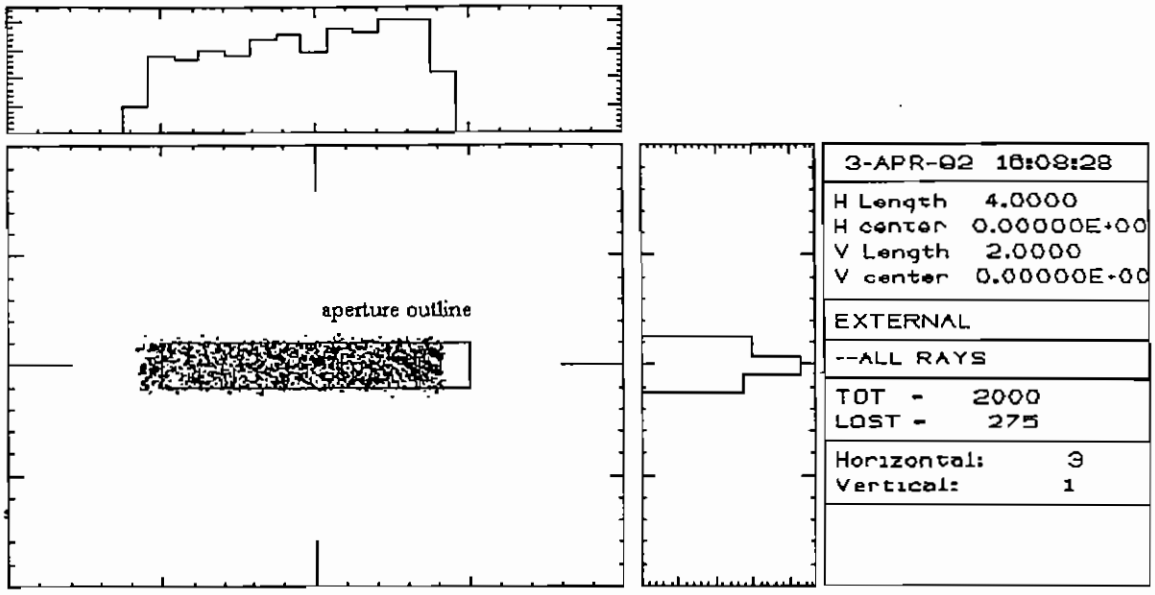

Figure 3(b) Image at 2mm monochromator entrance aperture for a 0.2mrad vertical source size

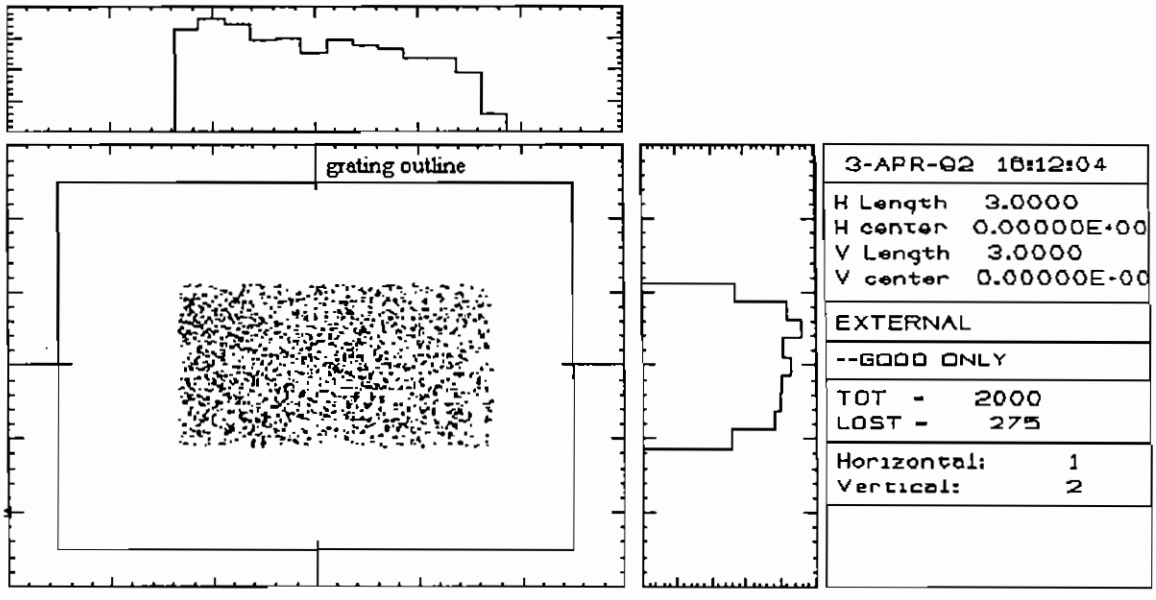

Figure 3(c) Footprint on grating at 140eV photon energy, 2mm aperture

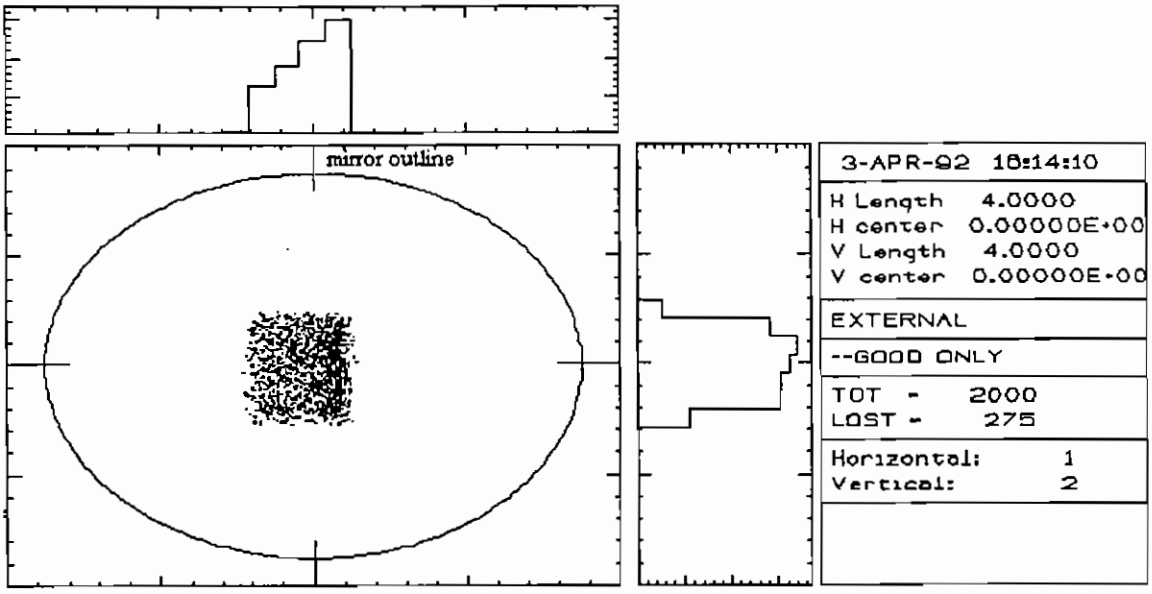

Figure 3(d) Foot print on spherical mirror at 140eV, 2mm aperture

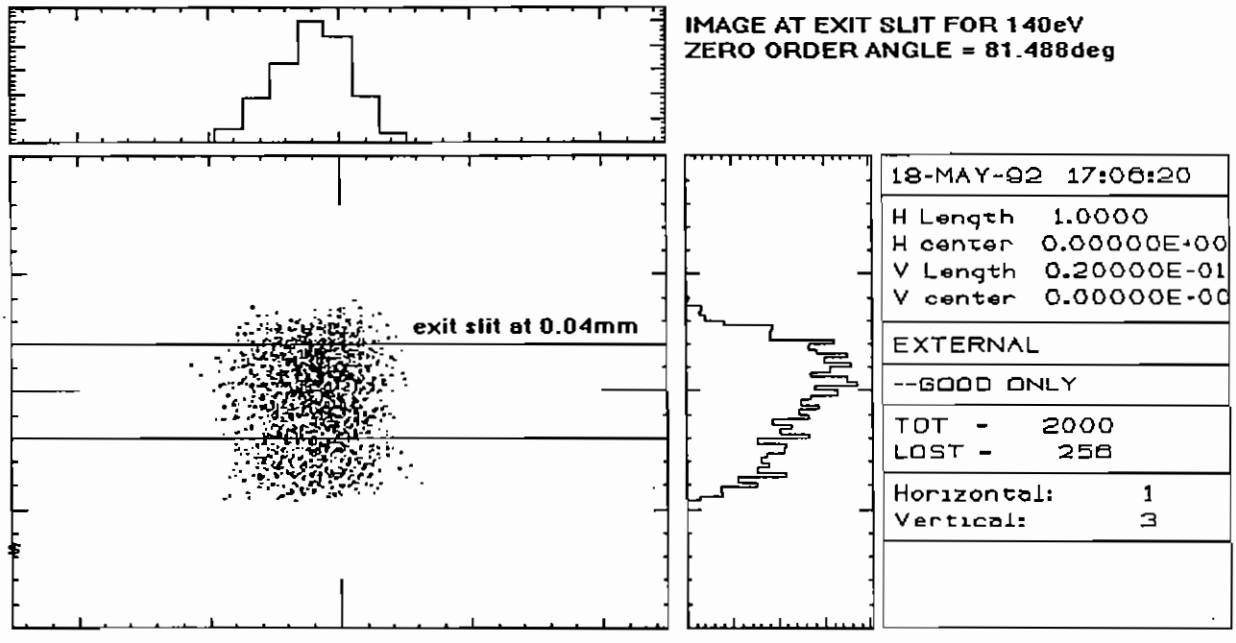

Figure 3(c) Image at exit slit for focus at zero order

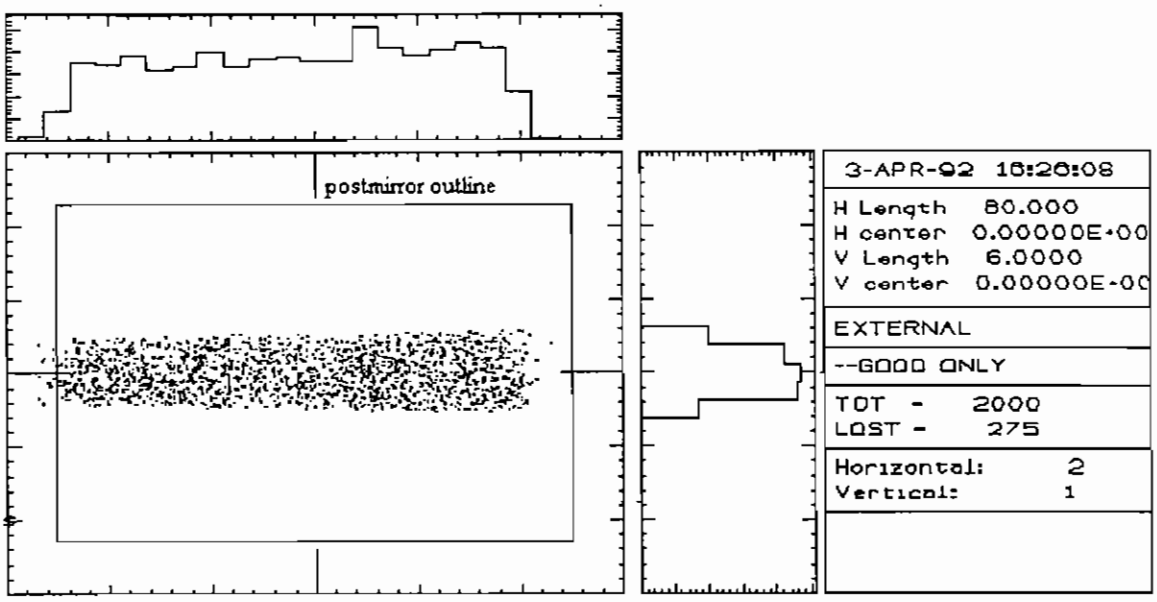

Figure 3(f) Footprint on postfocussing mirror at 140eV

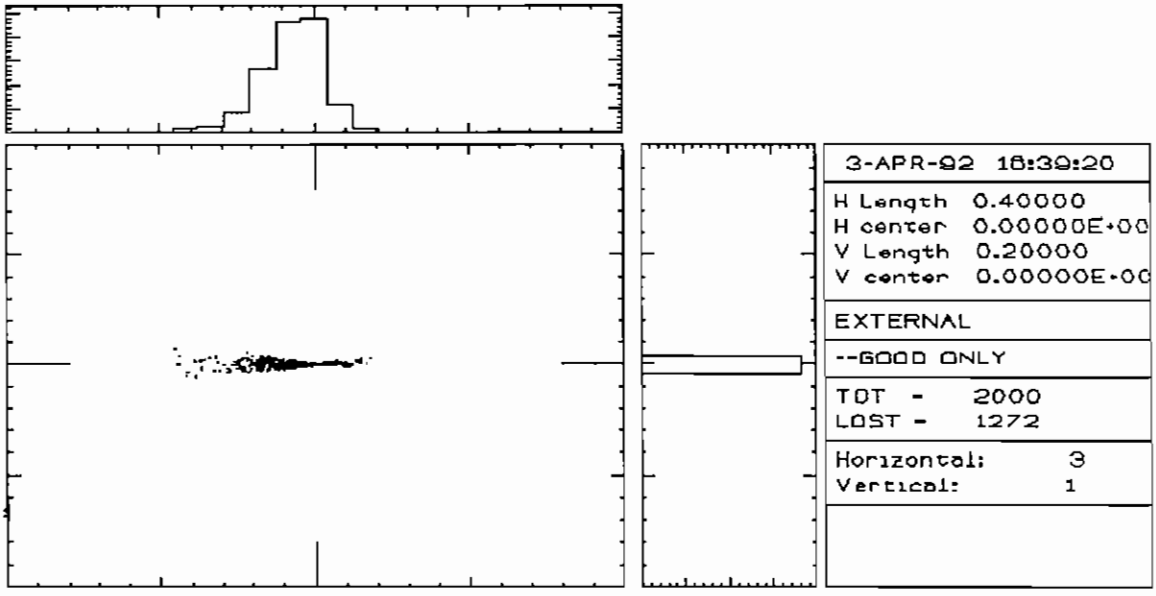

Figure 3(g) Image at sample for 140eV; vertical height=0.1mm; horizontal width=0.6mm

3. Focussing in a Miyake monochromator

3.1. Parallel light

If the light incident on the grating is parallel, then the monochromatic source point for the grating is infinity, and the paraxial focussing equation for the spherical mirror gives,

$$\frac{1}{\infty} + \frac{1}{lb} = \frac{2}{R\cos\theta} \qquad (1)$$

where lb is the mirror to slit distance, R is the radius of curvature, and θ is the zero order angle (and also the angle of incidence on the mirror).

The horizontal distance between the grating and exit slit is fixed and for a focus at the exit slits is given by,

$$y = \frac{R\cos\theta}{2} - X\cot 2\theta \qquad (2)$$

where X is the vertical distance between the grating and the mirror. This latter equation has two solutions for θ where y, X and R are fixed as in the present monochromator. Thus for each radius of curvature available there are two angles θ which focus the light at the exit slit, giving two different diffraction efficiencies vs. energy and in effect two different ranges of usable photon energy. These zero order (ZO) angles and corresponding mirror to exit slit distances, lb, are summarised in table 1.

TABLE 1

RANGE	ZO angle θ	ZO lb mm	MIRROR RADIUS
1	82.959 deg	203.2mm	3250mm
2	81.488 deg	321.3mm	4206mm
3	75.233 deg	567.5mm	4206mm
4	66.04 deg	708.9mm	3250mm

3.2. Divergent light

However, in the present arrangement the light cannot be considered to be parallel and the object distance in equation 1 is not infinity but P-L' where P is the distance from the grating to the mirror, and L' is the virtual source point

$$L' = -L\frac{\cos^2\beta}{\cos^2\alpha} \qquad (3)$$

where α and β are the angles of incidence and diffraction on the grating and are energy dependent (reference 5). L' varies from zero at the negative order horizon to infinity at the positive order horizon. At zero order, L' = L and the image is in focus for the zero order angles quoted in table 1.

If the monochromator is set up with these included angles (=2θ) then as the energy is scanned, the focus will move away from the exit slit and will not be in focus for monochromatic light resulting in a degradation of the resolution. The new focus position, lb, can be calculated from;

$$\frac{1}{P-L'} + \frac{1}{lb} = \frac{2}{R\cos\theta} \qquad (4)$$

3.3. Calculation of focus position using SHADOW

SHADOW has a utility called FOCNEW which can be used to produce plots of vertical image size (i.e. in the dispersive direction) versus distance from the exit slit position. Figure 4 gives a plot of vertical image size versus distance from the exit slit for 140eV photon energy and zero order angle = 81.488deg. which shows that the vertical focus is 1.47cm past the slit.

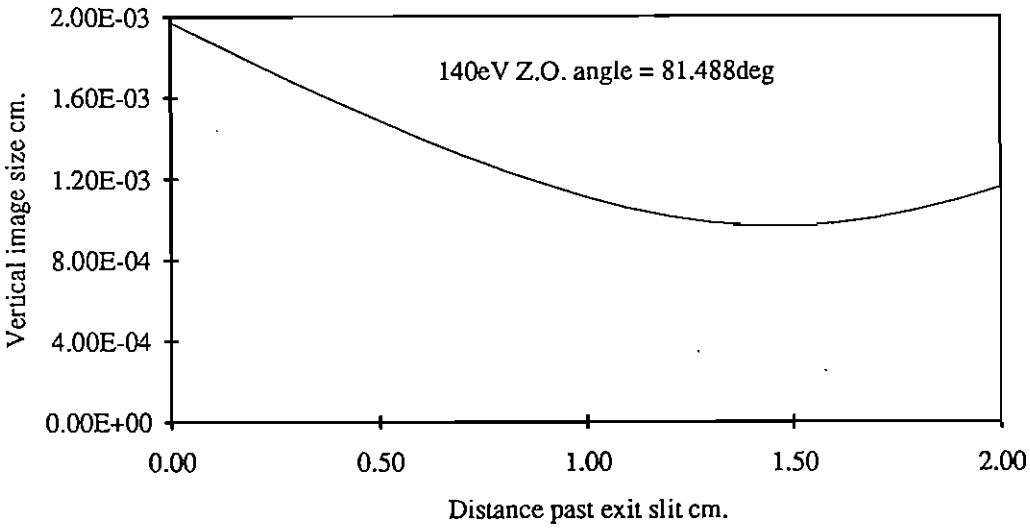

Figure 4. Variation of vertical image size with distance

3.4. Effect of changing included angle

Figure 5 shows how this mirror to focus distance, lb, changes with energy for two different zero order angles; 81.488deg. = focus at zero order; 80.95deg.= focus at exit slits for 154eV. Also plotted are mirror to focus distances derived from SHADOW. These agree to within 2mm with the distances derived from equation 4.

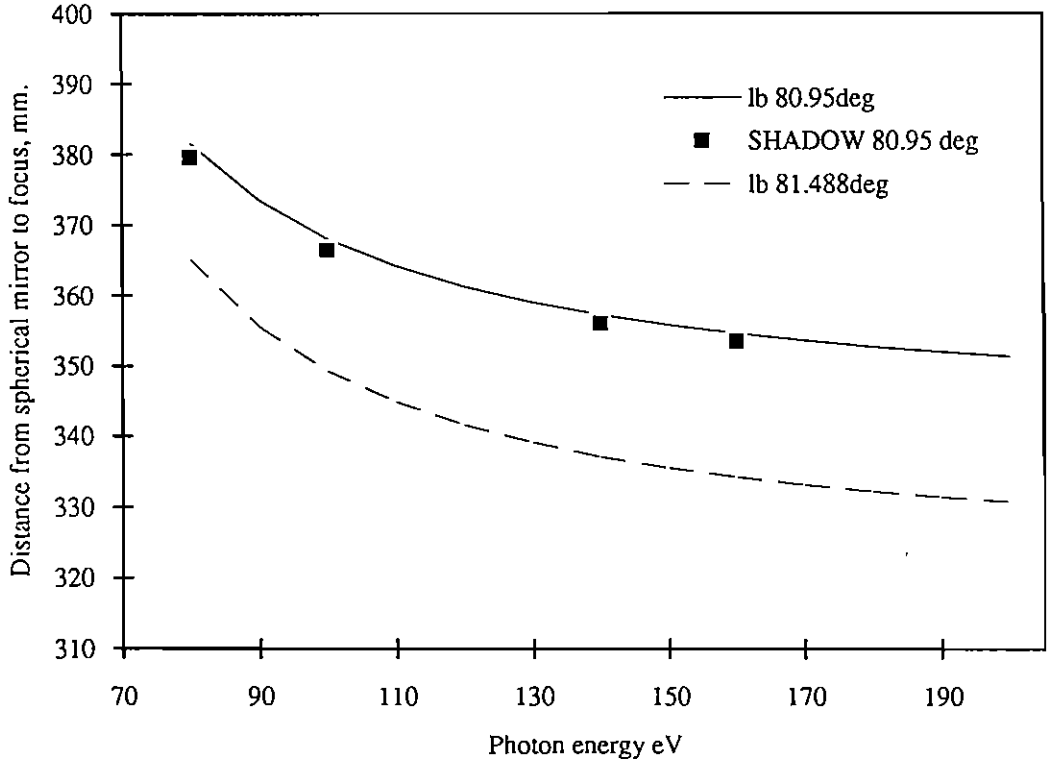

Figure 5. Variation of focus position with photon energy for two values of θ . The lines are derived from equation 4 and the data points are derived from SHADOW using FOCNEW.

Ideally for optimum resolution, the exit slits should be tracked along the beamline to the focus position for the desired photon energy. However, the exit slit position cannot be changed in this monochromator, but the mirror to slit distance and the included

angle 2θ are variable. From equation 41 in reference 3 given a fixed grating to slit distance, an included angle can be found for most photon energies which will produce a focus at the exit slits. These values of θ are plotted as a function of in-focus energy in figure 6. Note that here is no focus for the mirror with radius 4206mm (ranges 2 and 3) below 74.68eV, and for the second mirror radius 3250mm there is no focus below 21.38eV for the present grating to exit slit distance.

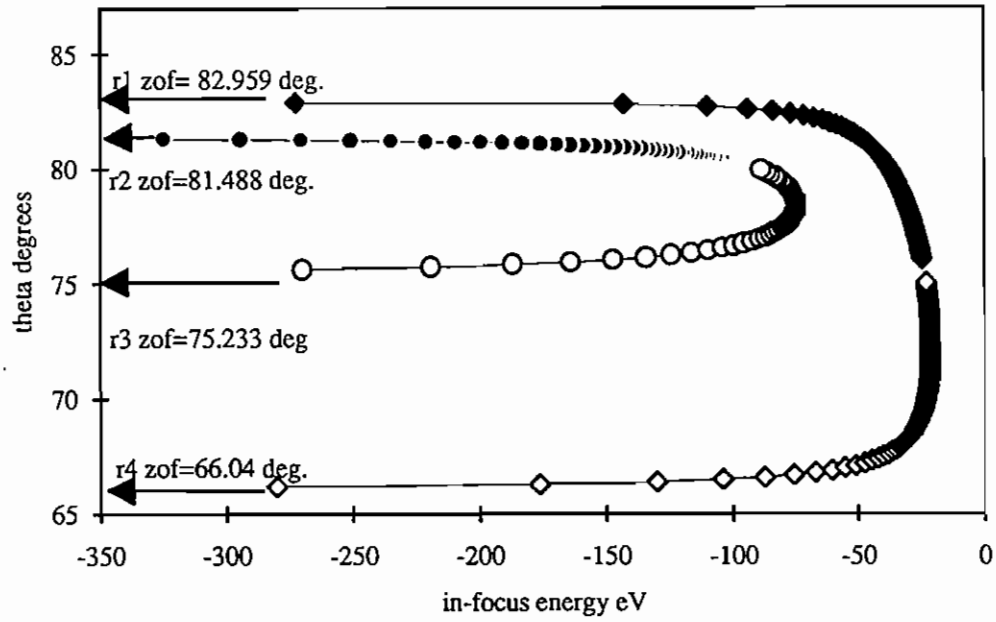

Figure 6. Plot of zero order angle, θ, as a function of in-focus photon energy. The negative value of the energy indicates that these angles give a focus in negative order. The system is constrained by the fixed grating to exit slit distance. The limits for θ as the photon energy increases are the values corresponding to focus at zero order, ZOF, listed in table 1.

Again, for optimum performance the included angle, 2θ, should be changed for each energy to keep the focus at the exit slits. This would involve rotating the spherical mirror and tracking it along the beamline. This is not practicable for the present monochromator. The operational mode used is to decide on a photon energy in the middle of the range to be in focus. This then fixes the included angle and the mirror to slit distance, lb.

For the commissioning in November '91, the zero order angle used for range 2 was 80.95deg giving lb=355.24mm and an in-focus energy of 154eV. The SHADOW image at the exit slit for 140eV photon energy is shown in figure 7. The improvement in image quality is clearly seen by comparison with figure 3(e).

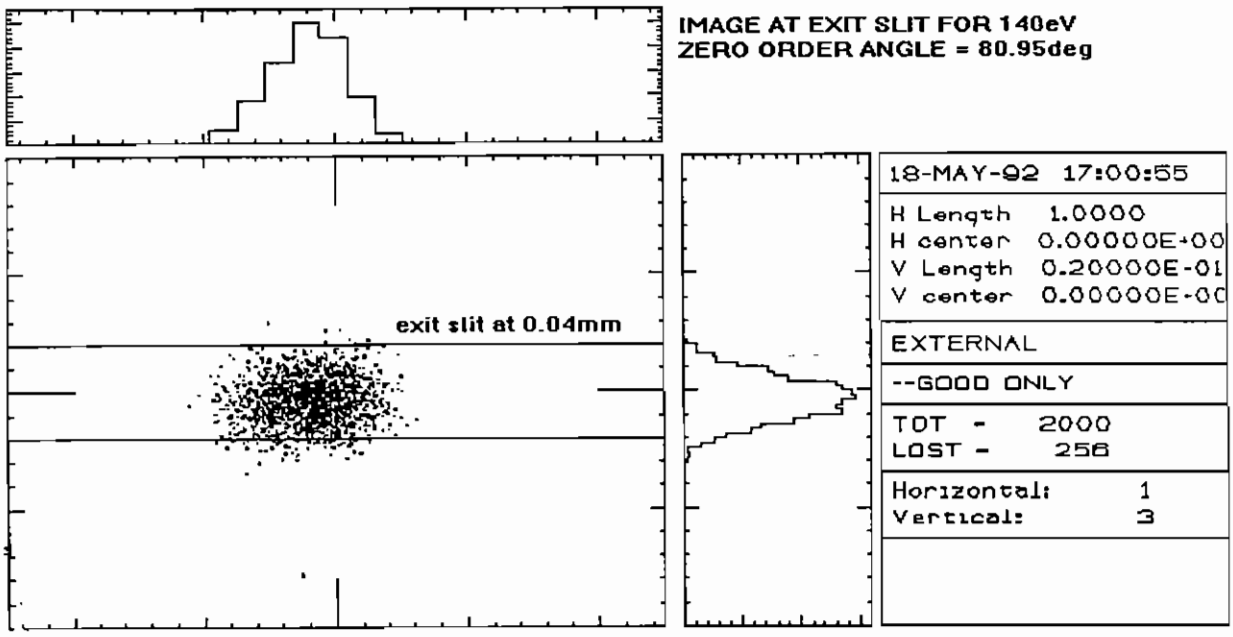

Figure 7. Effect of refocussing the monochromator on the image at the exit slits

The distance of the focus from the exit slit for the two zero order angles of interest is shown is figure 8. For θ=81.488deg the focus is never less than 10mm from the exit slits whereas for θ=80.95deg it is never more than 15mm away for the most commonly used photon energies, and for a significant part of the range is less than 5mm away.

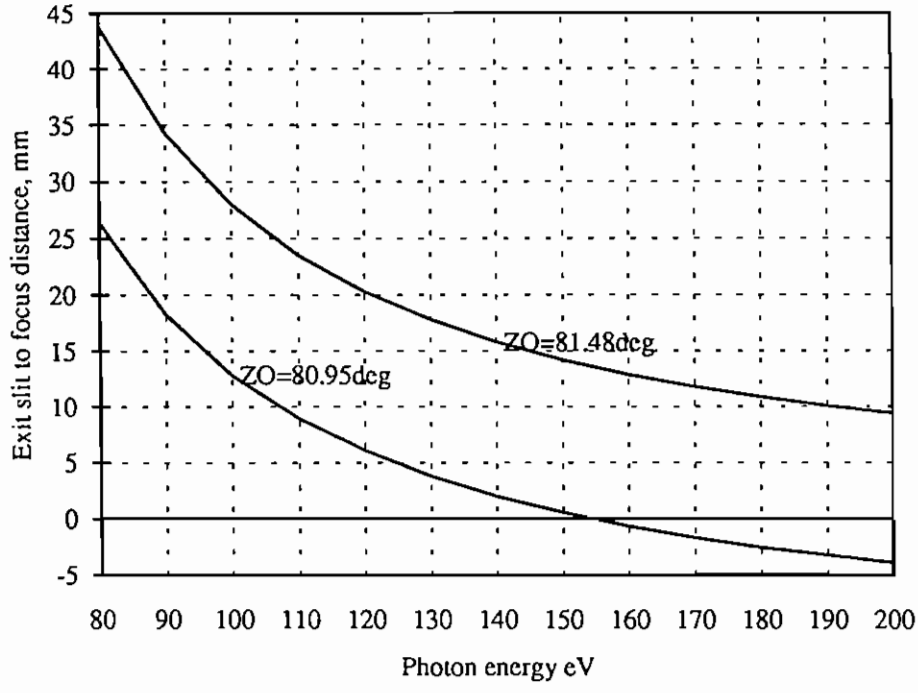

Figure 8. The distance of the focus from the exit slit is plotted as a function of photon energy for two zero order angles

4. Resolution

4.1. Resolution calculations using SHADOW

By using a ray source file with a broad range of energies centred on the tuned position for the monochromator (say 139.8eV to 140.2eV for the grating angle corresponding to 140eV), the bandpass at that energy can be calculated using a SHADOW utility called HISTO1. This produces a plot of number of rays against photon energy, such as that shown for 140eV in figure 3 (zero order angle 80.95deg.)

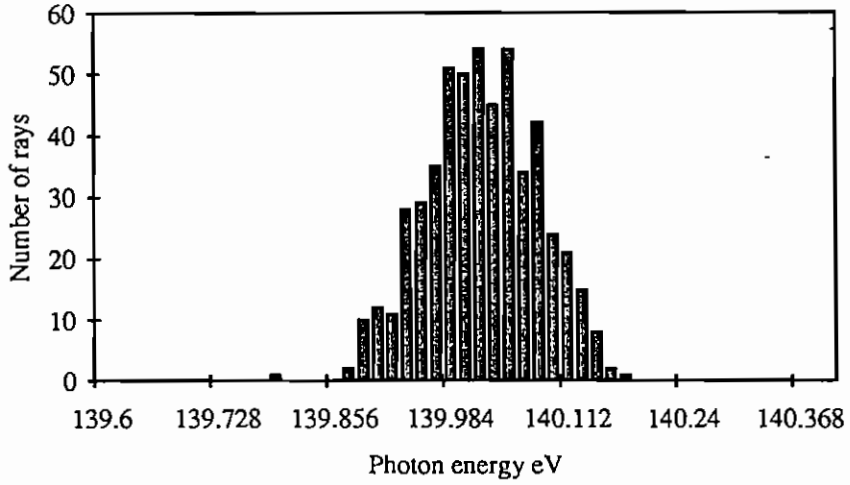

Figure 9. Output from HISTO1 showing the number of rays with a particular energy that pass through the exit slit of the monochromator.

The FWHM taken from these outputs were used to compare the resolution calculated from SHADOW to experimental data. Note that although the SHADOW source file contained the maximum 5000 rays, the HISTO1 output file only has a peak of 50. These poor statistics give an error in the FWHM of at most 10% for all the SHADOW results quoted here.

4.2. Resolution measurements

In Nov. '91 sets of resolution measurements were taken using a Cu(111) sample which could be cooled to LN_2 temperatures. The analyser used was a HA100. The spectra were curve fitted to find the FWHM equivalent of the Fermi edge. The experimental data have an error of +/- 10%. The monochromator was set up with zero order angles for focus at zero order (81.488deg) and for focus at 154eV (80.95deg).

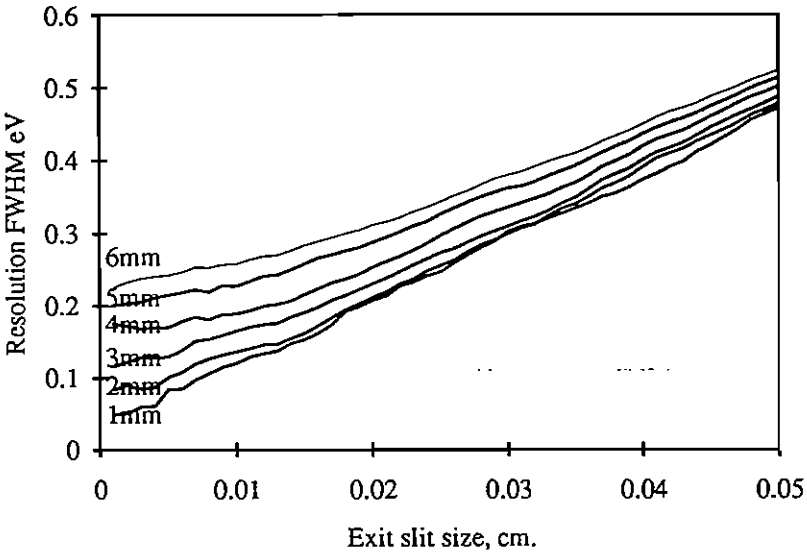

Figure 13(a). Calculated resolution versus exit slit size for six entrance aperture sizes at 80eV photon energy

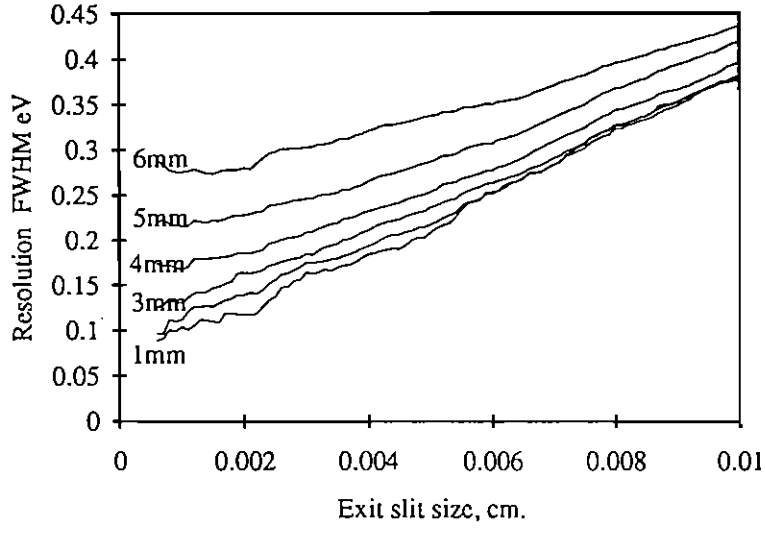

Figure 13(b) Calculated resolution versus exit slit size for six entrance aperture sizes at 140eV photon energy

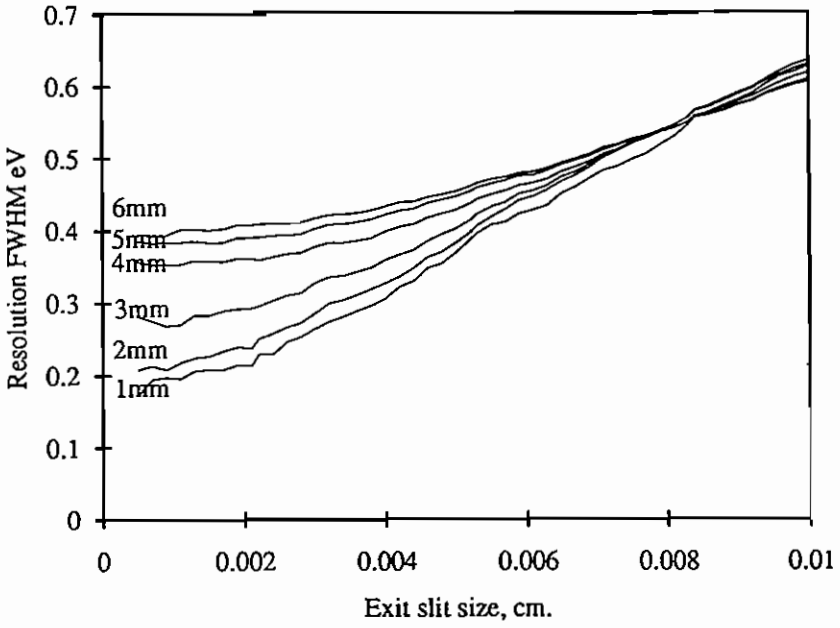

Figure 13(c). Calculated resolution versus exit slit size for six entrance aperture sizes at 180eV photon energy

The entrance slit limits the vertical angular acceptance and hence the fill of the spherical mirror. The image degradation due to coma is proportional to the square of the fill of this mirror while the degradation due to defocus is linearly proportional to this fill. The marked dependence on entrance slit size shows the system to be limited by coma (and at 80eV by defocus). Currently the larger apertures (>2mm) can only be used on ranges 3 and 4 due to the size of the grating and the aberration. Coma can be reduced by increasing the radius of curvature of the spherical mirror and to investigate this the system was traced for a 20m radius mirror. Figure 14 shows that the output of SLITS for 2mm(crosses) and 20mm(dashed line) entrance apertures are virtually identical.

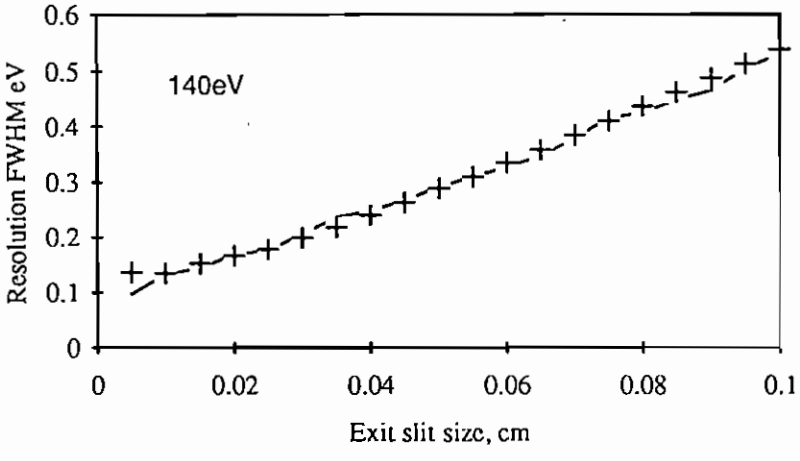

Figure 14. Resolution for a spherical mirror radius of 20m. and two entrance apertures: 2mm (crosses) and 20mm (dashed line).

However, the zero order angle for this system was chosen so that it focussed at 140eV. The dominant aberration is now defocus; the mirror to exit slit distance, lb, changes from 2.13m at 180eV to 2.328m at 140eV and 4.95m at 80eV compared to

changing by 0.03m for R=4.206m. It is impractical to consider tracking the exit slits by these distances. To benefit from the reduced coma, the defocus would also need to be removed by a more sophisticated premirror system such as that for 5U.1. This system keeps the virtual source distance, L', thus eliminating the problem of defocus (reference 6).

5. Summary

The plane grating monochromator on VUV6.1 has been raytraced using SHADOW and the results compared to commissioning data. The results agree well qualitatively and show how SHADOW can be used to predict the behaviour of optical systems.

The results show the benefits of reconfiguring the monochromator to reduce the defocus term. A further improvement could be gained by tracking the exit slits to the best focus for each energy, though it may be difficult to track exit slits of typically 0.04mm opening by the 40mm necessary.

Another benefit could be to use a spherical mirror of a much larger radius to reduce the effects of coma and allow larger entrance apertures to be used thus increasing the signal. However the system would need better preoptics to reduce defocus or would need to track the exit slits by at least 1m

6. Appendix 1:- Description of optical elements on beamline VUV6.1

element	figure	radius, cm	dist. to previous element, cm	incidence angle, degrees	blank mat.	size of active area, cm	coating
iris plate	rectangular aperture		39 before premirror			18.56 x 3.3	
premirror	cylindrical horiz.foc.	4677	700 to source	84.27065	SiC	56x 5 approx	platinum
aperture	rectangular					2 horizontal 0.1 to 0.6 vertical	
grating	plane	-------	32.6 to premirror	66.04 75.233 81.488 82.959	spectrosil	2.5 x 2.5	400 angs gold
spherical mirror	spherical; two inter-changeable mirrors	325 and 420.6	variable	66.04 75.233 81.488 82.959	spectrosil	3.5 diameter	400 angs gold
exit slit			variable, 85.7 to grating				
postmirror	ellipsoidal	160 semi-major 12.07 semi-minor	240 to exit slit 80 to sample	85	spectrosil	50 x 4.6	500 angs gold

7. References

1. S.Aksela et.al., Rev. Sci. Inst. 63 (1992) 1252
   E.Morikawa et al., Rev. Sci. Inst. 63 (1992) 1300

2. B.Lai and F.Cerrina, Nucl.Inst. Meth. A 246 (1986) 337
   B.Lai, K.Chapman and F.Cerrina, Nucl.Inst. Meth. A 266 (1988) 544
   C.Welnak et.al., Rev. Sci. Inst. 63 (1992) 865

3. H.A.Padmore, DL/SCI/TM45 (1986)

4. M.R.Howells, D.Norman, G.P.Williams, and J.B.West, J.Phys.E, Sci.Inst. 11 (1978) 199

5. M.V.R.K.Murty, J.O.S.A. 52 (1962) 768

6. C.S.Mythen, G.van der Laan and H.A.Padmore, Rev. Sci. Inst. 63 (1992) 1313